Proceedings World Geothermal Congress 2015
Melbourne, Australia, 19-25 April 2015

Nevado Del Ruiz Volcano (Colombia): A 3D Model Combining Geological and Geophysical Information

Javier González-Garcia[1], Juerg Hauser[2], David Annetts[2], José Franco[3], Edwin Vallejo[3], and Klaus Regenauer-Lieb[1,2]

[1]The University of Western Australia, 35 Stirling Ave, Crawley, WA, Australia.
[2]CSIRO, 26 Dick Perry Ave, Kensington, WA, Australia
[3]Servicio Geológico Colombiano, Diagonal 53 No 34-53, Bogota, Colombia

[1]javier.gonzalez@uwa.edu.au

Keywords: 3D, geological model, magnetotellurics, MT, volcano, Nevado del Ruiz, Colombia, Andes

ABSTRACT

The Nevado del Ruiz Volcano (NRV) in Colombia is a high-enthalpy geothermal system currently explored for its potential for energy production. We present a case study in the development of a 3D model of the NRV that integrates legacy geological, geochemical and seismic data with modern, newly acquired MT geophysical data. The initial geological interpretation is supported both by surface geology and published interdisciplinary conceptual models. Lithological and structural correlations in 3D space were obtained by using a potential field method. Inversions of geophysical data sets, such as magnetotellurics, were used to further constrain the model. The magnetotelluric dataset was acquired during a fieldwork campaign in 2013. For the first time, a full 3D geological characterisation of this volcanic system is publicly available, integrating and honouring the existing body of information. The spatial relationships proposed in the new model expand the current knowledge about the plumbing and hydrothermal system of the volcano. Magnetotelluric and seismic data interpretation is consistent with the existing conceptual model, which consists of a tripartite magma chamber beneath NRV interacting with a convective hydrothermal system on the W flank of the volcano, and with a steam heated aquifer beneath the NRV summit.

1. INTRODUCTION

The Nevado del Ruiz Volcano (NRV) is part of a volcanic massif located in Central Colombia (Figure 1). NRV is an active, andesitic stratovolcano that constitutes one of the northernmost manifestations of volcanism in the Andes Cordillera. It also hosts a sizeable hydrothermal system, inferred from numerous hot springs found across its vicinity. This hydrothermal system has been studied over the last decades as a potential geothermal energy resource; however, the location of a reservoir has not been publicly identified. The geological configuration of this region suggests strong structural control over the patterns of hydrothermal flow. This is evidenced by surface manifestations found almost exclusively along fault lines and intersections. Furthermore, a large proportion of the pre-volcanic basement consists of impermeable plastic rock, thus hindering the formation of a deep geothermal reservoir. This situation calls for 3D methods of visualisation to assess this geothermal resource, establishing spatial relationships between heat sources, flow patterns, lithology and fault networks.

This work intends to make a contribution to the public understanding of the volcanic and hydrothermal systems at NRV by offering a 3D interpretation of its geological configuration. A potential field interpolation method (Lajaunie et al., 1997; Calcagno et al., 2008) was used to create the 3D model. The model interpretation was based on geological cartography, (Mosquera et al., 1998; CHEC, 1983b), borehole data (Monsalve et al., 1998), a digital elevation model (http://earthexplorer.usgs.gov), a conciliation of previous published works, and the analysis of magnetotelluric and seismic data. The MT dataset used in this work is property of the Colombian Geological Survey, while the seismic dataset was generously provided by the Observatory of Vulcanology and Seismology of Manizales, Colombia.

2. REGIONAL SETTING

Volcanism in the study area is caused by the subduction of the Nazca Plate beneath the South American continent. The tectonic setting is influenced by the interactions of the Nazca, Caribbean and South American plates. The Northern Andes and Panama microplates lie along the major plate boundaries (cf. Bird, 2003). The stress regime in the region is transpressive, resulting from at least three major collision events, i.e. (1) the subduction of the Nazca plate to the west, (2) the subduction of the Caribbean plate to the north, and (3) the rigid indentation of the Panama block to the northwest (Cortés and Angelier, 2005). Differences in the velocity and angle of convergence of the interacting plates result in the superposition of two major shear stress components, i.e. 1) SW-NE compression caused by the collision of Nazca and the Northern Andes, and 2) NW-SE compression, due to the convergence of the Caribbean and Northern Andes.

Within the study area the transpressive stress regime is manifested as three distinctive sets of strike-slip faults. These sets are oriented N-S, NNE-SWW and NW-SE, respectively (Lopez, 2010). The kinematics of fault displacement is influenced by 1) the oblique convergence of the Nazca plate, resulting in right lateral displacement, and 2) by the rigid indentation of the Panama microplate, resulting in left lateral displacement (Ego et al., 1995; Taboada et al., 2000). The study area is located in a transitional region were the shear stress components are accommodated, favouring the coexistence of both right- and left- lateral fault kinematics.

Besides subduction, a series of crustal accretion events have shaped the configuration of the Northern Andes. Structurally, this region can be understood as a mosaic of exotic terranes bounded by suture faults (Etayo, 1986 *in* Gonzalez, 2001; Toussaint and Restrepo, 1996; Restrepo et al., 2011). The study area is located within the Tahami terrane. The terrane is a sliver of continental crust that was accreted to the main continent during Permian times. The Tahami terrane is traversed by the Palestina Fault, a

regional feature whose trace extends across a few hundred kilometres, and dates back to at least the Cretaceous period (Feininger, 1970). The Palestina Fault is thought to control the ascent of magma in NRV, and other neighbouring volcanoes, due to their alignment along its trace (Figure 1).

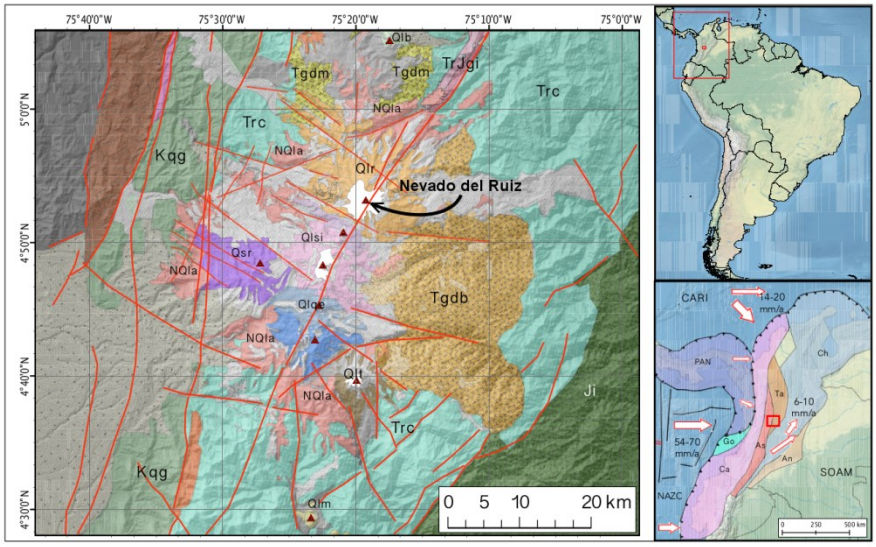

Figure 1: Geological map and tectonic context of the study area. A) Geological map. Data from Mosquera et al. (1998), CHEC (1983). (Trc: Cajamarca Complex; TrJgi: Gneissic Intrusive units; Ji: Ibague Batholith; Kqg: Quebradagrande Complex; Kar: Arquia Complex; Tgdm: Manizales Stock; Tgdb: El Bosque Batholith; NQla: Ancient Lavas; Qlb: Cerro Bravo Lavas; Qlr: Ruiz Lavas; Qlsi: Santa Isabel-El Cisne Lavas; Qsr: Santa Rosa Lavas; Qlqe: Quindio-Cerro España Lavas; Qlt: Tolima Lavas; Qlm: Machin Lavas). Fault traces (red) from Mejia et al. (2012) (PFS: Palestina Fault System, RFS: Romeral Fault System; OPFS: Otu-Pericos Fault System; TVM: Termales-Villamaria Fault; SR: Santa Rosa Fault). B) Tectonic map. Tectonic terrane boundaries from Restrepo et al. (2011) (Ta: Tahami Terrane, As: Allochthonous slivers of oceanic crust, Ch: Chibcha Terrane, Ca: Calima Terrane; CARI: Caribbean Plate, SOAM: South American Plate, NAZC: Nazca Plate, PAN: Panama microplate). Plate kinematics adapted from Freymueller et al. (1993), Trenkamp et al., (2002) and Restrepo-Moreno et al. (2009).

For the purposes of this study, the geological configuration of the region has been divided into two broad categories. The first category is the pre-volcanic basement, including the pre-existing materials present before the onset of modern volcanism. The second category is the volcanic cover, including the volcanic products that accumulated throughout the eruptive history of the region.

The prevolcanic basement is dominated by the Cajamarca Group, a polymetamorphic complex composed of four distinct members (CHEC, 1983; Gonzalez, 2001). The most widespread of these is the pellitic member, formed by mica schists, phyllites and meta-sediments. The other members occur as isolated pockets or lenses of variable extension. Among these, are the mafic member, composed of greenschists and amphibolites; the calcareous member, composed of marble and calc-schists; and the siliceous member, composed of quartzites and quartz-schists. These rocks are derived from marine sediments that accumulated c. 240-220 Ma ago in a syn-rift basin that formed after the Pangean breakup (Villagomez et al., 2011). Subsequently, these sediments underwent regional metamorphism in an Andean-type orogen c. 230-218 Ma ago (Restrepo et al., 2011). The actual thickness of the Cajamarca Group in the study area remains undetermined.

To the west of the study area, the Romeral Fault System puts in contact the Cajamarca Group and the Quebradagrande Complex. Based on a regional gravity anomaly, this fault system has been interpreted as a suture zone separating oceanic terranes to the west from continental terranes to the east (Barrero, 1979 in Forero-Suarez, 1990). On the other hand, the Quebradagrande Complex has been interpreted as a Cretaceous volcanic arc that accreted to the continent (Pindell and Kennan, 2009; Villagomez and Spikings, 2012).

The Cajamarca Group has been intruded by multiple igneous bodies. In the study area, the oldest of such intrusions are grouped within the Gneissic Intrusive bodies. These intrusives have either amphibolitic or felsic composition, and are found alongside the Palestina Fault (CHEC, 1983; Gonzalez, 2001). The age of these rocks has been estimated as 207±5 Ma, for the felsic gneisses, and 200 ± 40 Ma, for the amphibolites (Vesga and Barrero, 1978 in CHEC, 1983). Furthermore, there are two other intrusive bodies in the area of interest. These intrusions were caused by post-tectonic magmatism in the early stages of the Andean Orogeny during the Eocene (Gonzalez, 2001; Restrepo-Moreno et al., 2009). This is the case of the Manizales Stock, a massive quartz-diorite located to the NE of the study area, which has been dated as 62.4±3.6 Ma old (Brook, 1984 in Aspden et al., 1987). The other Eocene intrusion is El Bosque Batholith, a predominantly granodioritic massive body located to the SE of the study area. The age of the batholith has been estimated as 49±1.7 Ma (Vesga and Barrero, 1984 in Aspden et al., 1987). The chronologic and petrologic similarities, together with their spatial proximity, has led some authors to propose that these two bodies are part of one single batholith (Gonzalez, 2001).

Modern volcanism began approximately 3 Ma ago. Thouret et al. (1990, 1995) recognised four different stages of volcanic development. First, a Pre-volcanic stage (c. 3.00-1.25 Ma ago) was characterised by two pyroclastic events and one lava flow. Second, an Ancestral stage (c. 1.8-0.4 Ma ago) was characterised by a constructive phase, including the formation of a broad stratovolcano, followed by a destructive stage including events of caldera collapse. Third, an Older stage (c. 0.76-0.04 Ma ago) was characterised by an alternation of constructive and destructive periods. Fourth, a Recent stage (c. 0.1 Ma ago-Present) is characterised by multiple constructive and destructive periods. Currently, volcanism undergoes a destructive stage characterised by the formation of pyroclastic products.

The current model for the magmatic system of NRV consists of a tripartite magma chamber (Melson et al., 1990; Londoño and Sudo, 2002; Stix et al., 2003). A main reservoir of basaltic magma, at ~10 km depth, feeds an intermediate chamber of dacitic composition, at ~6 km depth. This intermediate reservoir in turn is connected to a shallow andesitic chamber at ~2 km depth. The magmatic conceptual model is presented in Figure 2a.

The hydrothermal conceptual model includes two separate systems, separated by a silicic carapace (Sturchio et al., 1988; Giggenbach et al., 1990; Larios-Lopez, 1992). Above the carapace, meteoric waters percolate from the glacier moving downslope through the volcanic cover. Beneath the carapace, there is a high-enthalpy system that interacts with the magma chambers. The hydrothermal conceptual model is presented in Figure 2b.

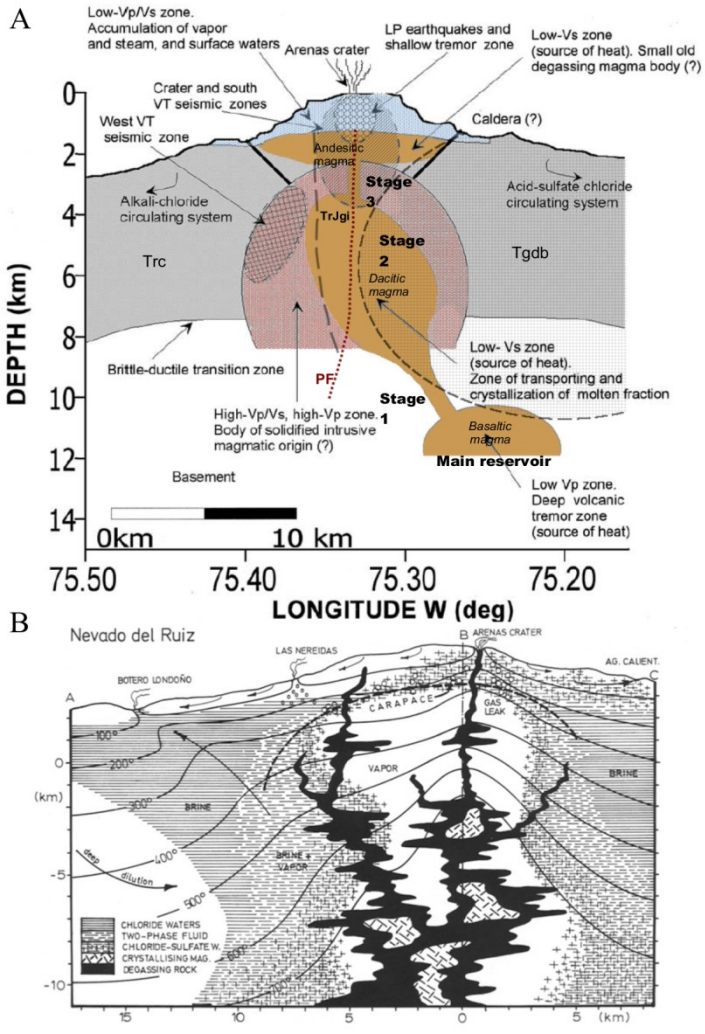

Figure 2: Conceptual model for A) the magmatic system, and B) the hydrothermal system at NRV. A) Tripartite model proposed by Londoño and Sudo (2002). The original figure has been modified to indicate the stages of magmatic ascent proposed by Stix et al. (2003) and the chamber dominant composition proposed by Melson et al. (1990). The inferred geological contacts are drawn. B) Potential distribution of fluids based on geochemical information, taken from Giggenbach et al. (1990).

3. MAGNETOTELLURIC ANALYSIS

3.1 Data acquisition

A new magnetotelluric dataset was obtained in the field; it contains 43 stations with a frequency range between 10,000-0.1 Hz. The equipment employed consisted of two recording units Phoenix V8, with triplets of induction coils type MTC-80 and AMTC-30, and non-polarising electrodes type PE4. The stations were set in a cross-shaped dipole arrangement, with a 50 m dipole length. The lengths of the recorded time series were 90 minutes for the AMTC-30 coils, and at least 16 hours for the MTC-80 coils. The study area is located in a sparsely populated region inside a national park, and no major indications of cultural noise were registered in

the data. The station layout formed a circuit around the base of the NRV, with an average separation between stations of 1 km. Simultaneously-recording stations were deployed at least 5 km apart. The station layout and selected profile trace are shown in Figure 3.

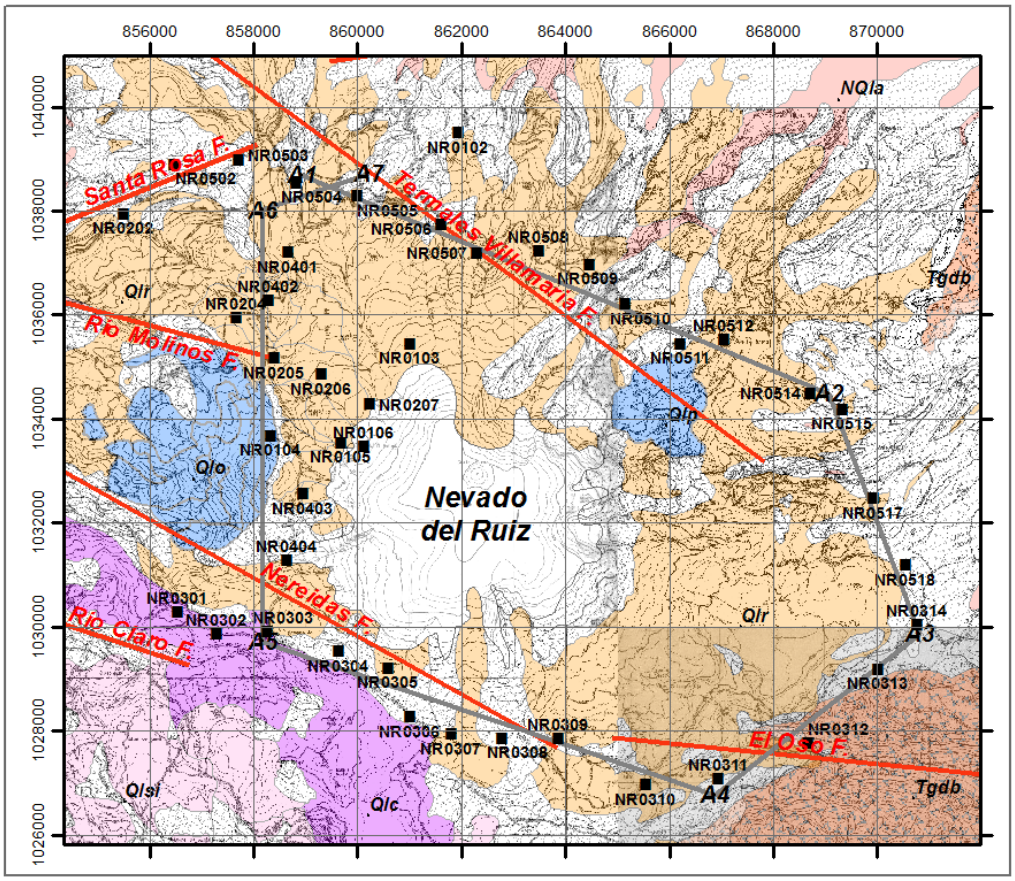

Figure 3. Location of the magnetotelluric stations and profiles used in this study.

3.2 Data processing

The time series for each component of the electromagnetic field were windowed and converted into the frequency domain. Four evaluation frequencies per decade were used. Robust processing was applied to the Fourier coefficients to obtain the transfer functions (i.e. impedance tensor and tipper vector) at each location. The remote reference method (Gamble et al., 1979) was employed to mitigate coherent noise. However, given the low level of signal contamination, the results do not show much variation from single-station processing. For each evaluation frequency, robust processing results in a population of 100 cross powers. Subsequently, outliers were removed manually from that population. The remaining values were stacked together, yielding the estimated values of the transfer functions. These transfer functions are expressed in terms of apparent resistivity and phase shift, calculated from the antidiagonal elements of the impedance tensor. The antidiagonal elements correspond to the decoupling modes of the electromagnetic field (i.e. the Zxy component represents the transverse electric mode, TE, while the Zyx component represents the transverse magnetic mode, TM). Data processing was implemented using the standard software from Phoenix Geophysics.

3.3 Modelling

The values of apparent resistivity and phase shift for both decoupling modes were plotted as a function of frequency. Subsequently, the effects of galvanic distortion caused by minor near-surface sources were removed applying the method described by Bibby et al. (2005). This method was implemented by using the library MTpy (Krieger, Peacock, Inverarity; Adelaide, 2013). Smooth curves were fit through the corrected data for both TE and TM modes. These curves were obtained by applying the D+ solution method (Parker, 1980; Beamish and Travassos, 1992).

The smooth curves for apparent resistivity and phase were used to obtain Occam 1D models (Constable et al., 1987). Smooth model curves were calculated with an error threshold of 5%. Simple 1D layered models were estimated from those model curves, by comparing the forward response that adjusts as closely as possible to the smooth D+ curves. Inversion was applied multiple times to these layered models until a stable model consistent with prior knowledge was obtained.

Subsequently, the non-linear conjugate gradient algorithm (Rodi and Mackie, 2001) was used to apply 2D MT inversion along a selected profile (Figure 3). The D+ curves, together with the tipper vectors were used as input parameters. The initial model was a homogeneous halfspace with a resistivity value of 100 Ωm. Convergence was achieved with a root mean square value of 2.54. The 2D model results are presented in Figure 4.

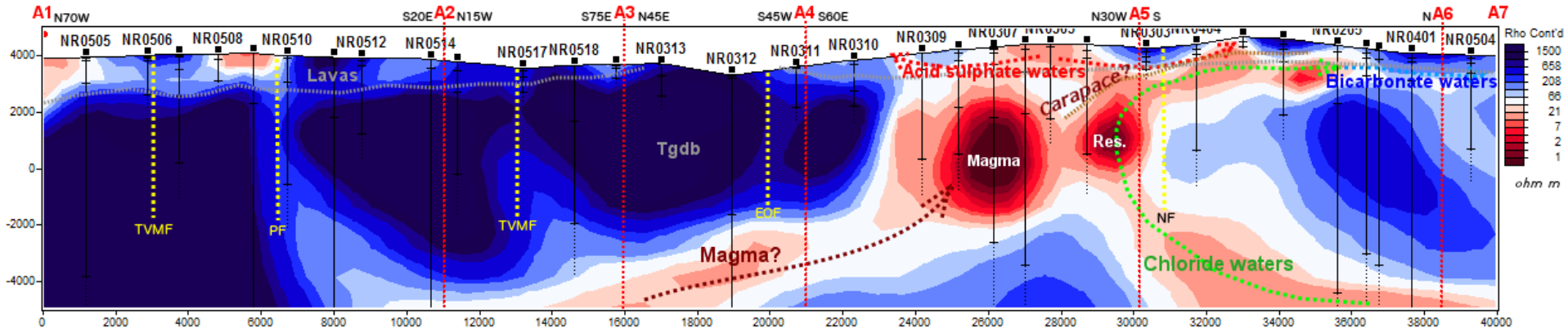

Figure 4. Results from 2D inversion of MT data along perimetric section A (location in Figure 3). The resistivity anomalies appear to be consistent with the conceptual models from Figure 2. A major conductor is observed along segment A4-A5, which is interpreted as the intermediate magma chamber from the conceptual model in Figure 2A. Another conductor is observed along segment A3-A4, and is interpreted as a deep magmatic chamber located beneath the resistive El Bosque Batholith (Tgdb). A C-shaped conductor, outlined by the green dotted line, is observed along sections A4-A5-A6. That conductor resembles the deep convective hydrothermal system proposed by Giggenbach et al. (1990) (Figure 2B). The highly conductive region at the inflection point is interpreted as a permanent reservoir, adjacent to the magma chamber, and possibly contained by a solid carapace composed of precipitated silica and clay minerals (cf. Giggenbach et al., 1990). This carapace would separate the deep convective system from circulating shallower acid sulphate waters. The yellow dotted lines represent the fault planes intersecting the cross section. A subtle resistivity contrast between 2000-3000 m.a.s.l. is interpreted as the depth to the pre-volcanic basement. The MT dataset was acquired in collaboration with the Colombian Geological Survey.

4. SEISMIC CATALOGUE ANALYSIS

A catalogue of approximately 42000 volcanotectonic microseismic events recorded by the Observatory of Vulcanology and Seismology of Manizales between 2001 and 2014 was analysed. The purpose of this analysis was to identify seismogenic regions that could be associated with movements of magma, indicative of active chambers. The first step was to remove from the catalogue those events either with a horizontal or vertical error greater than 1000 m or with RMS error greater than 0.2. A dataset of 40161 events was selected, and is contained within the mapped area in Figure 3. That region was discretised into cubic voxels of 250 m side length, which is close to the mode values for the error distribution of the dataset (Figure 5).

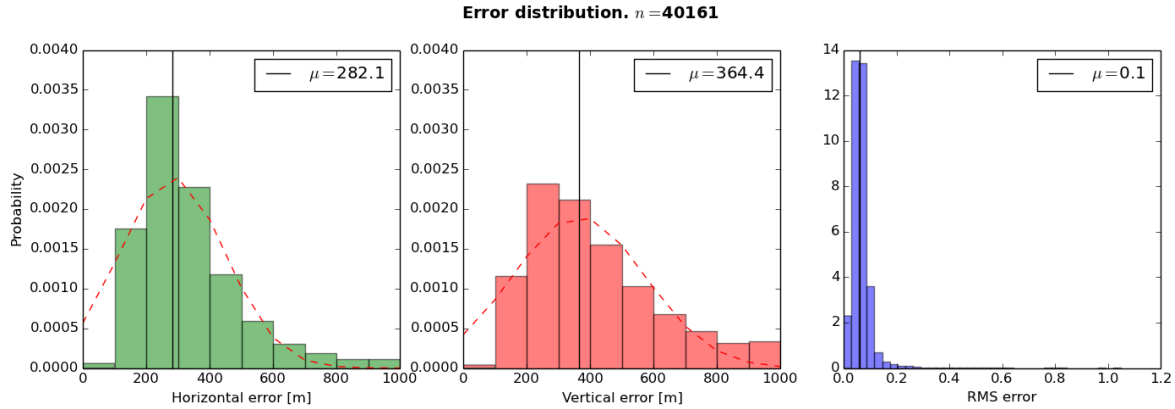

Figure 5. Histograms representing the error distribution of a seismic catalogue of volcanotectonic events registered in the NRV between 2001 and 2014. Events with location errors greater than 1 km or with RMS greater than 0.2 were removed. The dataset was provided by courtesy of the Observatory of Vulcanology and Seismology of Manizales.

Once the model space has been discretised, seismicity is quantified within each voxel. Each seismic event is then represented by a spheroid, centred at the hypocentre and with semiaxes given by the respective horizontal and vertical errors (Figure 6). The voxels contained or intersected by the spheroid are assigned a value equal to the number of their vertices within the spheroid divided by 8, i.e. the total number of vertices in a voxel (e.g. 1 contained vertex corresponds to a value of 0.125, while 2 vertices correspond to 0.25, etc.). The values assigned to each event are normalised, allowing a cumulative value of 1 per event across the affected voxels. The same process is then repeated for all the events and the same value is calculated for each voxel. The value associated to quantifying the amount of microseismicity occurring at a given voxel is hereafter referred as seismic rate. This seismic rate value is calculated by dividing the voxel accumulated value by the total number of events used. High seismic rate values are interpreted as indicative of areas where an active magma chamber is more likely to be present (i.e. stages 2 and 3 in Figure 9). This observation is consistent with prior knowledge for this volcanic system.

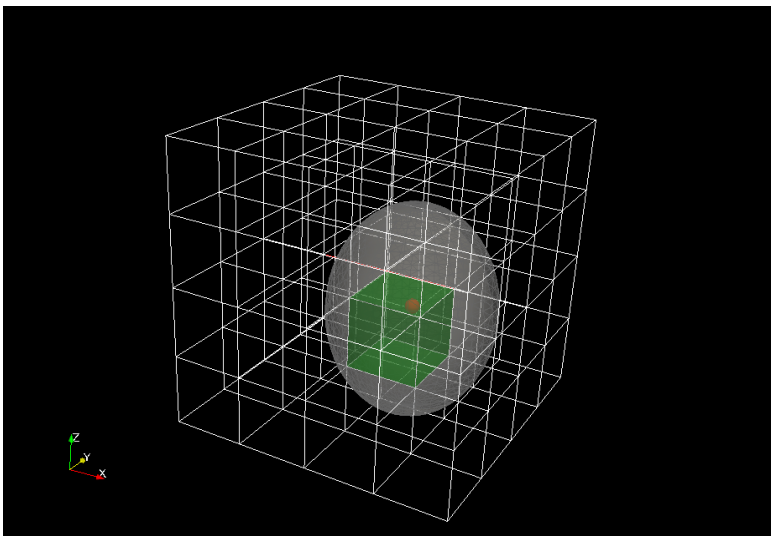

Figure 6. Spheroidal representation of seismic events used to quantify seismic rate values within each voxel.

5. 3D GEOLOGICAL MODEL PREPARATION

The potential field method (Lajaunie et al., 1997) was used to represent the 3D geological interpretation of the NRV. In this method, the geometry of geological units is simulated by means of implicit surfaces. The potential field approach requires the definition of a series of scalar potentials that represent the geology in the model domain. The method is described in detail in the works of Lajaunie et al. (1997), Chilès et al. (2004), Aug et al. (2005) and Calcagno et al. (2008). The implementation is carried out using the software *Geomodeller/Editeur Geologique* (BRGM and Intrepid Geophysics). The program requires as inputs 1) a digital elevation model, 2) geological interface location data, 3) orientation data, and 4) stratigraphic and structural relationship information.

The digital elevation model was obtained from the USGS Earth Explorer server (http://earthexplorer.usgs.gov). The geological interface data was digitised from geological maps at scales 1:1,000,000 (Gomez-Tapias et al., 2007) y 1:100,000 (Mosquera et al., 1998; CHEC, 1983). Lithological borehole records from the well Nereidas-1 (Monsalve et al., 1998) were included. Orientation data was not readily available in the study area, and was inferred from indirect observations. The modelled faults include Romeral Fault System, dividing the whole model; Palestina, affecting the upper crust; and other local faults (e.g. Termales-Villamaria, Nereidas, Rio Claro, Rio Molinos), affecting the brittle crust.

The geological model was designed at two different scales. The first scale includes regional features and its areal extent is the same as the map in Figure 1. The model domain has a lateral extension of 70x70 km, with a maximum depth of 35 km. The results are shown in Figure 7. The second scale focuses on the NRV, with an extension of 28x45 km (Figure 8).

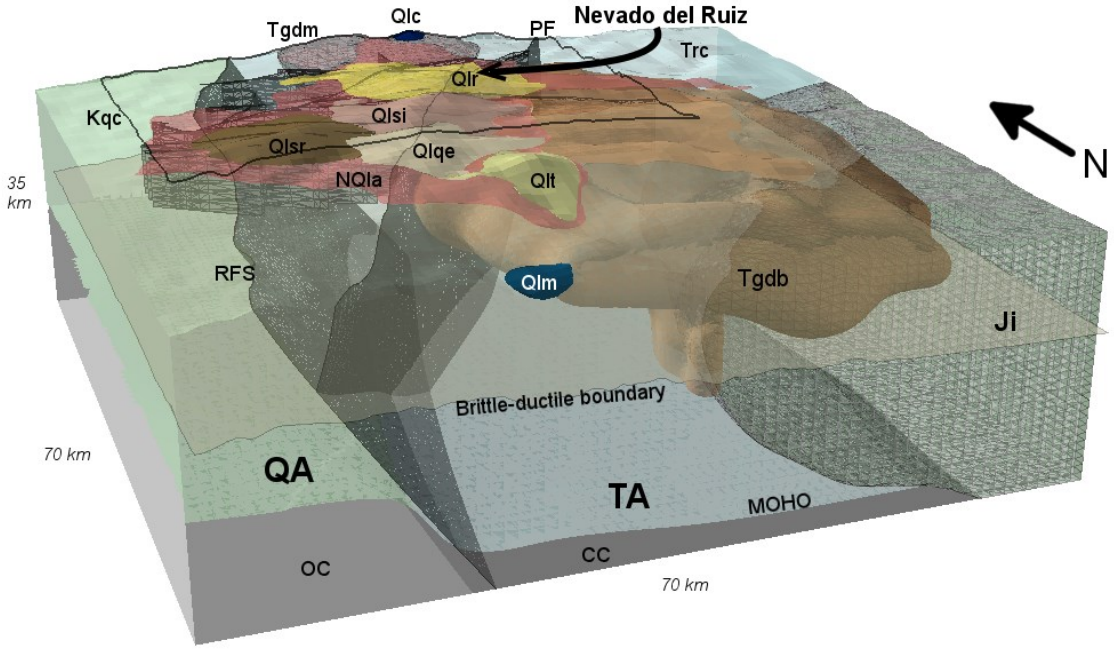

Figure 7. Geological model, regional scale. Model domain corresponds to the area of the map in Figure 1. Black rectangular area represents the domain of the model in Figure 8. Model obtained using the software Geomodeller. (Trc: Cajamarca Complex; TrJgi: Gneissic Intrusive units; Ji: Ibague Batholith; Kqg: Quebradagrande Complex; Tgdm: Manizales Stock; Tgdb: El Bosque Batholith; NQla: Ancient Lavas; Qlr: Ruiz Lavas; Qlsi: Santa Isabel-El Cisne Lavas; Qlsr: Santa Rosa Lavas; Qlqe: Quindio-Cerro España Lavas; Qlt: Tolima Lavas; Qlm: Machin Lavas). Fault traces (red) from Mejia et al. (2012) (PF: Palestina Fault System, RFS: Romeral Fault System; TVM: Termales-Villamaria Fault; SR: Santa Rosa Fault).

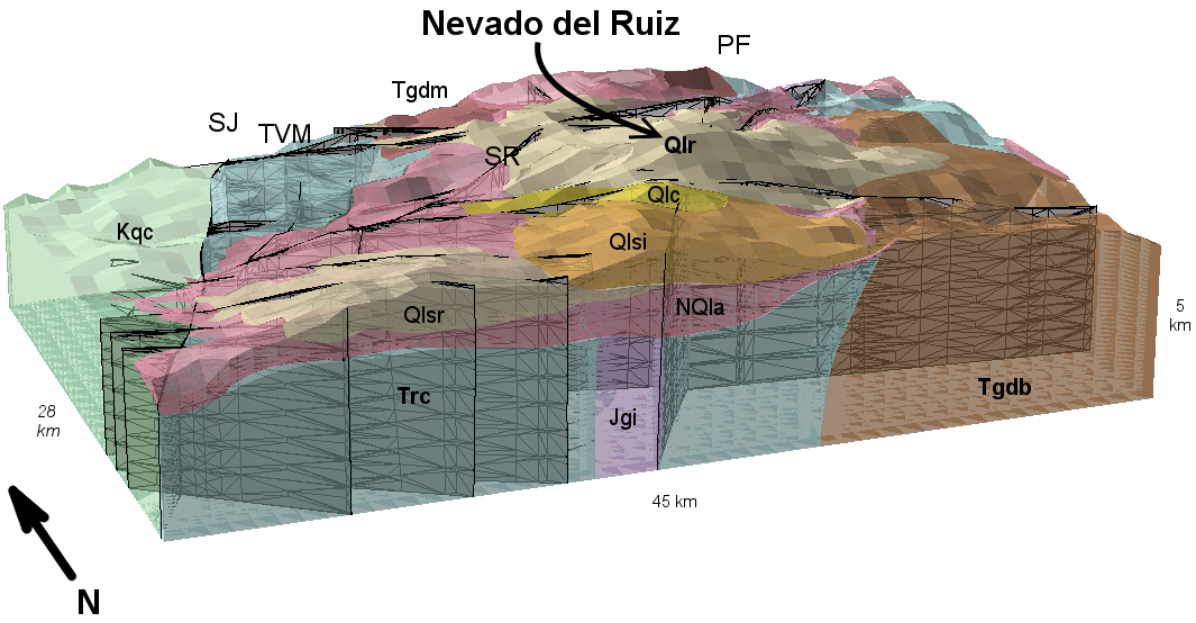

Figure 8. Geological model, local scale. This scale focuses on the Nevado del Ruiz Volcano. Model obtained using the software Geomodeller.

6. DISCUSSION

The interpretation of magnetotelluric and seismic data appears to be consistent with prior conceptual models of the hydro-magmatic system at NRV (Figure 2). Inversion of magnetotelluric data suggests that a deep convective hydrothermal system exists in the W flank of the volcano, in the vicinity of the Nereidas Fault (Figures 4 and 9). The same dataset allows identifying a strong conductor in the S flank of NRV. This conductor coincides with the expected location of the intermediate magma chamber (i.e. stage 2) described in the diagram in Figure 2A. Additionally, a deep conductor was identified in the SE flank of the volcano beneath a strong resistor. This configuration suggests that a deep magmatic reservoir exists towards the base of El Bosque Batholith, corresponding to magmatic stage 1 from the conceptual model.

The seismogenic zones identified from the volcanotectonic event catalogue also support the existence of an intermediate magma chamber in the S flank. Furthermore, a large seismogenic region beneath the summit of NRV is interpreted as the shallow magma chamber from the tripartite system (i.e. stage 3). This region is located beyond the cover of the MT survey and was not detected by this method. The seismogenic zones interpreted from the event catalogue represent those regions of space with a maximum likelihood of finding a magma chamber (i.e. stages 2 and 3 in Figure 9).

Additionally, a subtle resistivity contrast is observed in areas covered by lavas at elevations between 2000 and 3000 m.a.s.l. (Figure 4, segments A1-A2-A3 and A4-A5-A6-A7). That contrast is interpreted as the bottom of the Ancient Lava unit (NQla), which marks the pre-volcanic basement discontinuity.

A convective hydrothermal system is developed around the heat source composed of the tripartite magma chamber. That hydrothermal system has a deep root, with an upflow zone where chloride waters interact with the intermediate, dacitic chamber. The presence of the intermediate magma chamber to the south of NRV creates an asymmetric convective system with an outflow zone moving to the north and northwest. Hydrothermal flow appears to be channelled across the fault network formed by the Nereidas, Termales-Villamaria and Santa Rosa faults, as well as along the pre-volcanic basement discontinuity. The deeper portion of the outflow zone retains chloride composition, whereas the shallower portion interacts with the host rock evolving into bicarbonate waters. The chloride waters that migrate across the Nereidas Fault eventually reach the surface at the Botero-Londoño hot springs, west of the study area. The acid sulphate waters would be associated to a vapour-dominated region above the shallow magma chamber. These acid waters are also channelled across the fault network, flowing closer to the surface and mixing with meteoric waters. It is possible that a cap seal of precipitated silica and clay minerals forms at the outer margins of the convective system, creating a semipermeable barrier that prevents water mixing, allowing however the escape of volatile gases (cf. Figure 2B).

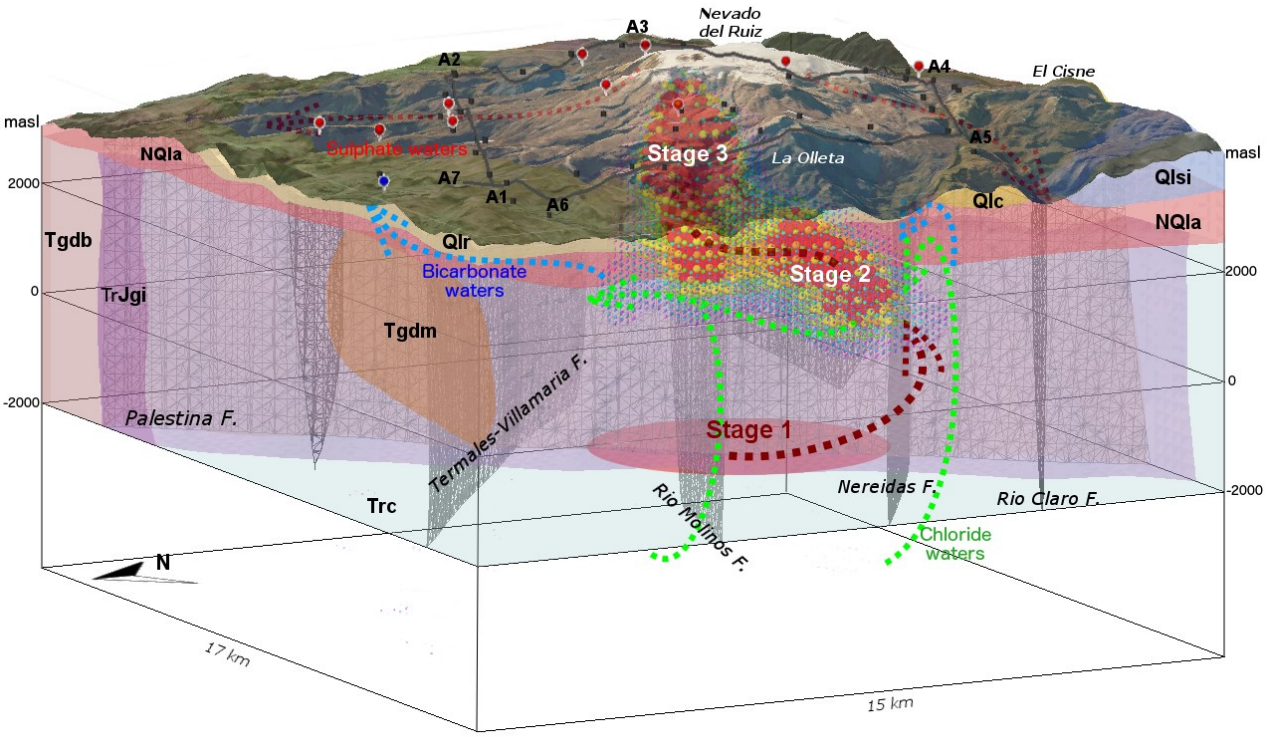

Figure 9. 3D visualisation of the conceptual model of the NRV geothermal system. This conceptual model is supported by 2D inversion of MT data and the identification of seismogenic regions based on a catalogue of volcanotectonic seismic events. Location of hot springs (droplets) after Alfaro et al. (2002). The convective hydrothermal systems are represented by dotted arrows (red: acid sulphate waters, blue: bicarbonate waters, green: chloride waters). Magmatic ascent patterns represented by brown arrows. The modelled area corresponds to the map in Figure 3. The seismic data was provided by courtesy of the Observatory of Vulcanology and Seismology of Manizales.

7. CONCLUSIONS

A 3D geological model was developed for the Nevado del Ruiz Volcano. The offered interpretation is consistent with the existing body of knowledge, and was constrained with magnetotelluric and seismic data. A tripartite magmatic chamber was identified beneath the summit of the NRV. A large convective hydrothermal system interacts with the magma bodies, while its flow pattern is structurally controlled by the fault planes of the Nereidas, Rio Molinos, Santa Rosa and Termales Villamaria faults and by the pre-volcanic basement discontinuity.

ACKNOWLEDGEMENTS

Special mention is made to those organisations that have contributed towards the execution of this project. Funding has been provided by the Australian Development Scholarship Awards program, from the Australian Government. Technical support has been provided by CSIRO. Logistical support during fieldwork was provided by the Colombian Geological Survey. On the individual level, we express our gratitude for the feedback received from Dr. Florian Wellmann on the use of 3D modelling software, and Thomas Hoskin on processing of MT data. Also, we highly appreciate the collaboration from the South Australian Centre for Geothermal Energy Research at the University of Adelaide. During the acquisition of MT data, the efforts of Patricia Ponce, Adriana Ortega, Fabio Gomez and Luis Ruiz were crucial to the successful completion of the campaign. Similarly, a mention of gratitude is made to Claudia Alfaro, John M. Londoño and Gloria Cortés from the Colombian Geological Survey.

REFERENCES

Alfaro, C., Aguirre, A., & Jaramillo, L. (2002). Inventario de Fuentes Termales en el Parque Nacional Natural de Los Nevados. Ingeominas, 1–101.

Aspden, J. A., McCourt, W. J., & Brook, M. (1987). Geometrical control of subduction-related magmatism: the Mesozoic and Cenozoic plutonic history of Western Colombia. Journal of the Geological Society, 144(6), 893–905.

Beamish, D., & Travassos, J. M. (1992). The use of the D+ solution in magnetotelluric interpretation. Journal of Applied Geophysics.

Bibby, H. M., Caldwell, T. G., & Brown, C. (2005). Determinable and non-determinable parameters of galvanic distortion in magnetotellurics. Geophysical Journal International, 163(3), 915–930. doi:10.1111/j.1365-246X.2005.02779.x

Bird, P. (2003). An updated digital model of plate boundaries. Geochemistry Geophysics Geosystems, 4(3), 1027–. doi:10.1029/2001GC000252

Calcagno, P., Chilès, J.-P., Courrioux, G., & Guillen, A. (2008). Geological modelling from field data and geological knowledge: Part I. Modelling method coupling 3D potential-field interpolation and geological rules. Physics of the Earth and Planetary Interiors, 171(1), 147–157.

CHEC. (1983a). Final Report. In Investigación Geotérmica Macizo Volcánico del Ruiz (Vol. 1, pp. 1–127). Bogotá: Central Hidroeléctrica de Caldas.

CHEC. (1983b). Investigación Geotérmica Macizo Volcánico del Ruiz.

Chilès, J. P., Aug, C., Guillen, A., & Lees, T. (2004). Modelling the geometry of geological units and its uncertainty in 3D from structural data: the potential-field method. Orebody Modelling and Strategic Mine Planning.

Constable, S., Parker, R., & Constable, C. (1987). Occam's inversion: A practical algorithm for generating smooth models from electromagnetic sounding data. Geophysics, 52(3), 289–300.

Cortés, M., & Angelier, J. (2005). Current states of stress in the northern Andes as indicated by focal mechanisms of earthquakes. Tectonophysics, 403(1), 29–58.

Ego, F., Sebrier, M., Lavenu, A., Yepes, H., & Egues, A. (1996). Quaternary state of stress in the Northern Andes and the restraining bend model for the Ecuadorian Andes (Vol. 259, pp. 101–116). Presented at the Tectonophysics.

Feininger, T. (1970). Palestina-Fault,Colombia. Geological Society of America Bulletin, 81(4), 1201–&.

Forero Suarez, A. (1990). The basement of the Eastern Cordillera, Colombia: An allochthonous terrane in northwestern South America. Journal of South American Earth Sciences, 3(2), 141–151.

Freymueller, J. T., Kellogg, J. N., & Vega, V. (1993). Plate motions in the North Andean region. Journal of Geophysical Research: Solid Earth (1978–2012), 98(B12), 21853–21863.

Gamble, T. D., Goubau, W. M., & Clarke, J. (1979). Magnetotellurics with a remote magnetic reference. Geophysics, 44(1), 53–68.

Giggenbach, W., García P, N., Londoño C, A., Rodriguez, L., V, Rojas G, N., & Calvache, M., V. (1990). The chemistry of fumarolic vapor and thermal-spring discharges from the Nevado del Ruiz volcanic-magmatic-hydrothermal system, Colombia. Journal of Volcanology and Geothermal Research, 42(1), 13–39.

Gomez-Tapias, J., Nivia-Guevara, A., Montes-Ramirez, N., Jiménez-Mejía, D., Tejada-Avella, M., Sepúlveda-Ospina, M., et al. (2007). Mapa Geológico de Colombia. Ingeominas.

González, H. (2001). Planchas 206 y 225. Manizales-Nevado del Ruiz. Ingeominas, 1–93.

Lajaunie, C., Courrioux, G., & Manuel, L. (1997). Foliation fields and 3D cartography in geology: Principles of a method based on potential interpolation. Mathematical Geology, 29(4), 571–584. doi:10.1007/BF02775087

Larios-Lopez, D. (1992, December 1). The hydrothermal system of Nevado del Ruiz Volcano, Colombia. The Louisiana State University.

Leuangthong, O., & Deutsch, C. V. (Eds.). (2005). 3D Geological Modelling and Uncertainty: The Potential-Field Method. In Geostatistics, Banff 2004 (Vol. 2, pp. 145–154). Springer.

Londoño, J. M., & Sudo, Y. (2002). Velocity structure and a seismic model for Nevado del Ruiz Volcano (Colombia). Journal of Volcanology and Geothermal Research, 119(1-4), 61–87.

Mejía, E. L., Velandia, F., Zuluaga, C. A., López, J., & Cramer, T. (2012). Análisis estructural al noreste del Volcán Nevado del Ruiz, Colombia-Aporte a la exploración geotérmica. Boletín De Geología UIS, 34(1), 27–41. doi:10.1029/2003TC001551

Melson, W., Allan, J., Jerez, D., Nelen, J., Calvache, M., Williams, S. N., et al. (1990). Water contents, temperatures and diversity of the magmas of the catastrophic eruption of Nevado del Ruiz, Colombia, November 13, 1985. Journal of Volcanology and Geothermal Research, 41, 97–126.

Monsalve, M., Rodriguez, G., Mendez, R., & Bernal, N. (1998). Geology of the Well Nereidas 1, Nevado Del Ruiz Volcano, Colombia. Geothermal Resources Council Transactions, 22.

Mosquera, D., Marín, P., Vesga, C., & González, H. (1998). Geología de la plancha 206. Ingeominas.

Parker, R. L. (1980). The inverse problem of electromagnetic induction: existence and construction of solutions based on incomplete data. Journal of Geophysical Research: Solid Earth (1978–2012), 85(B8), 4421–4428.

Pindell, J. L., & Kennan, L. (2009). Tectonic evolution of the Gulf of Mexico, Caribbean and northern South America in the mantle reference frame: an update. Geological Society.

Restrepo, J. J., Ordóñez Carmona, O., Armstrong, R., & Pimentel, M. M. (2011). Triassic metamorphism in the northern part of the Tahamí Terrane of the central cordillera of Colombia. Journal of South American Earth Sciences, 32(4), 497–507. doi:10.1016/j.jsames.2011.04.009

Restrepo-Moreno, S. A., Foster, D. A., Stockli, D. F., & Parra-Sánchez, L. N. (2009). Long-term erosion and exhumation of the "Altiplano Antioqueño," Northern Andes (Colombia) from apatite (U–Th)/He thermochronology. Earth and Planetary Science Letters, 278(1), 1–12. doi:10.1016/j.epsl.2008.09.037

Rodi, W., & Mackie, R. L. (2001). Nonlinear conjugate gradients algorithm for 2-D magnetotelluric inversion. Geophysics, 66(1), 174–187. doi:10.1190/1.1444893

Stix, J., Layne, G. D., & Williams, S. N. (2003). Mechanisms of degassing at Nevado del Ruiz volcano, Colombia. Journal of the Geological Society, 160(4), 507–521. doi:10.1144/0016-764902-028

Sturchio, N. C., Williams, S. N., Garcia, N. P., & Londono, A. C. (1988). The hydrothermal system of Nevado del Ruiz volcano, Colombia. Bulletin of Volcanology, 50(6), 399–412.

Taboada, A., Rivera, L. A., Fuenzalida, A., Cisternas, A., Philip, H., Bijwaard, H., et al. (2000). Geodynamics of the northern Andes: Subductions and intracontinental deformation (Colombia). Tectonics, 19(5), 787. doi:10.1029/2000TC900004

Thouret, J. C., Cantagrel, J., Robin, C., Murcia, A., Salinas, R., & Cepeda, H. (1995). Quaternary eruptive history and hazard-zone model at Nevado del Tolima and Cerro Machin volcanoes, Colombia. Journal of Volcanology and Geothermal Research, 66(1-4), 397–426.

Thouret, J. C., Cantagrel, J., Salinas, R., & Murcia, A. (1990). Quaternary eruptive history of Nevado del Ruiz (Colombia). Journal of Volcanology and Geothermal Research, 41(1-4), 225–251.

Trenkamp, R., Kellogg, J. N., Freymueller, J. T., & Mora, H. P. (2002). Wide plate margin deformation, southern Central America and northwestern South America, CASA GPS observations. Journal of South American Earth Sciences, 15(2), 157–171.

Villagómez, D., & Spikings, R. (2012). Thermochronology and Tectonics of the Central and Western cordilleras of Colombia: Early Cretaceous–Tertiary evolution of the Northern Andes. Lithos, 160-161, 228-249. doi: 10.1016/j.lithos.2012.12.008

Villagómez, D., Spikings, R., Magna, T., Kammer, A., Winkler, W., & Beltrán, A. (2011). Geochronology, geochemistry and tectonic evolution of the Western and Central cordilleras of Colombia. Lithos, 125(3-4), 875–896. doi:10.1016/j.lithos.2011.05.003